

Colloidal HgTe Nanocrystals with Widely Tunable Narrow Band Gap Energies: From Telecommunications to Molecular Vibrations

Maksym V. Kovalenko,* Erich Kaufmann, Dietmar Pachinger, Jürgen Roither, Martin Huber, Julian Stangl, Günter Hesser, Friedrich Schäffler, and Wolfgang Heiss

Institute of Semiconductor and Solid State Physics, Johannes Kepler University, Linz A-4040 Linz, Austria

Received December 22, 2005; E-mail: maksym.kovalenko@jku.at

For the visible¹ and the near-IR² spectral region, a multitude of highly luminescent wide-gap semiconductor nanocrystals (NCs) have been chemically synthesized. Despite the enormous success of colloidal NCs, used, for example, in lasers,³ as fluorescent markers⁴ in biological systems, or in single photon sources,⁵ the development of NCs with tunable IR emission up to wavelengths of more than 3 μm is still challenging.⁶ Hg chalcogenides are most appropriate to obtain *narrow band gaps* from NCs in the quantum confinement regime because their bulk constituents exhibit zero band gaps, whereas those of all alternative binary narrow gap semiconductors, such as lead chalcogenides and group III antimonides, are at least 0.18 eV (InSb, 300 K).⁷

So far, the best synthetic routes to Hg chalcogenide NCs are those based on thiol-capping in aqueous medium.^{8,9} The optical characterization of NCs in aqueous solutions is, however, restricted to the near-IR, due to the opaqueness of water at wavelength $> 1.3 \mu\text{m}$. Synthetic approaches to HgTe¹⁰ NCs in the organic solvents suffered from the high reactivity, instability, and tendency to uncontrolled growth, even at temperatures as low as 70–100 °C. Therefore, we have synthesized HgTe NCs in aqueous solutions and transferred them to organic solvents by a ligand-exchange procedure. By the choice of the stabilizer, we optimized the growth dynamics, the luminescence quantum yields (up to 40%), and the phase transferability. As a result, we obtain stable HgTe NCs, giving room temperature emission which is strongly size-tunable between the wavelength of 1.2 and 3.7 μm .

The HgTe NCs were prepared in aqueous solutions via a room temperature reaction between $\text{Hg}(\text{ClO}_4)_2$ and H_2Te gas (bubbled through) in the presence of the hydrophilic thiols, thioglycerol (TG), thioglycolic acid (TGA), L-cysteine, mercaptoethanol (ME), and mercaptoethylamine (MEA), as stabilizers (see Supporting Information for details). To achieve a continuous generation of H_2Te gas, we make use of a specially designed electrochemical cell as a cheap and convenient source. There, the electrochemical reduction of elemental Te in acidic solution results in an efficient (current yield ~ 0.6) generation of H_2Te gas. To push the emission of HgTe NCs to longer wavelength, their sizes were increased by a postsynthetic heat-treatment, typically at 75–80 °C. Subsequently, the ligand exchange with dodecanethiol (DT), a hydrophobic thiol, was carried out. The structural characterization and size determination of the NCs were done by wide-angle X-ray diffraction (XRD) and transmission electron microscopy (TEM).

For all used stabilizers, the as-synthesized HgTe NCs have almost identical sizes of 3–4 nm and PL peak wavelength between 1.1 and 1.3 μm . The choice of the initial hydrophilic capping thiol, however, is crucially important for controlling the growth dynamics at elevated temperatures, for the transferability from the aqueous to the organic phase, and for the optical properties of larger HgTe NCs. All results discussed in the following are restricted to MEA- and TG-stabilized NCs since they provide the highest PL quantum

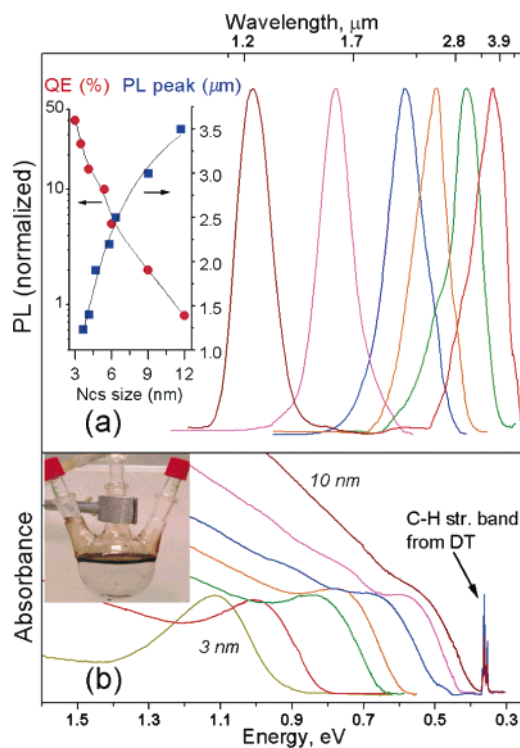


Figure 1. Representative room temperature PL (a) and absorption (b) spectra of DT-capped HgTe NCs in CCl_4 . The insets show the size dependence of the PL peaks with the corresponding quantum efficiencies (a) and illustrate the phase transfer completeness for MEA used as initial stabilizer (b).

efficiencies (QE) and the same range of PL tuning. As shown in the inset of Figure 1a, the PL peak wavelength can be shifted from 1.2 to 3.5 μm by increasing the nanocrystal average size from 3 to 12 nm. In particular, the PL peak energy as a function of diameter d (nm) is well approximated by $E[\text{eV}] = 0.3 + 0.2d^{-1} + 5.7d^{-2}$. By comparing the evolution of the PL peaks with growth time, we observe a much faster growth rate for MEA-capped particles than for TG-capped ones (Figure S2). For the largest NCs, emission up to 4 μm is observed, thus the luminescence overlaps with the molecular vibration band of the stabilizer, shown in Figure 1b. For these long wavelengths, the quantum efficiency (QE) is found to be on the order of 0.5–2%, while it increases up to 40% for the near-IR, similar to that demonstrated for oleic acid-capped PbSe NCs.⁶ The HgTe NCs retain their luminescence properties when they are incorporated into polymers, such as poly(methyl methacrylate) (Figure S3), which is of high importance for future applications. A similar tuning behavior as that for the PL is observed by the linear absorption spectra (Figure 1b). In the near-IR, they show well-resolved peaks corresponding to the lowest electronic transitions and a broadening of them with increasing particle size.

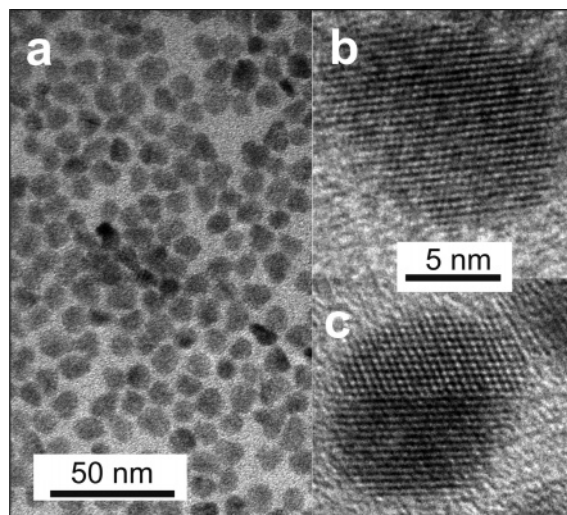


Figure 2. TEM image of ~ 9 nm DT-capped HgTe NCs emitting at $3 \mu\text{m}$ (a). High-resolution TEM images of single crystal (b) and twinned (c) particles.

One important advantage of the MEA-capped HgTe NCs is their extremely high transferability from the aqueous to the organic phase. Previously, Gaponik et al.¹² have established that an efficient phase transfer of thiol-capped CdTe NCs needs rather high amounts of DT and acetone to be added to achieve a large interface area between the aqueous and the organic phase (moderately stable emulsion). We observe a very similar behavior for the TG, TGA, and ME-capped HgTe NCs with transfer efficiencies typically $\leq 80\%$. In contrast, the phase transfer of MEA-capped HgTe NCs is completed in time scales of seconds after the injection of a small amount of DT (as low as 1/8 of the volume of the aqueous phase), as illustrated in inset of Figure 1b. This enables a facile, virtually one-pot synthesis of large amounts of hydrophobic HgTe NCs. Between the transferability and the colloidal stability of aqueous HgTe NCs, a correlation is observed, indicating that the ligand exchange is strongly influenced by the binding energy between Hg atoms at the nanocrystal surface and the thiol (see Supporting Information).

The structural characterization by TEM and XRD shows the high crystallinity of the HgTe NCs, as well as their uniformity in size and regularity in shape (Figure 2). Most HgTe NCs are predominantly formed as defect-free single crystals (Figure 2b). A few percent of the NCs, however, show interesting planar defects, such as twins (Figure 2c) and stacking faults (Figure S4). The heat-treatment of HgTe NCs increases the occurrence of planar defects and broadens the size distribution of NCs from ~ 10 to $\sim 30\%$. The latter was successfully refined to $\sim 10\%$ by size-selective precipitation. Like HgTe bulk (coloradoite),¹² the NCs have the zinc blende crystal structure, as is determined by the XRD patterns in Figure 3, and by indexing the dot-rings in the selected-area electron diffraction (SAED) patterns (Figure S5). The effect of finite size broadening is clearly seen in all XRD peaks.

In conclusion, we demonstrate a facile aqueous-based synthesis of high-quality HgTe NCs with widely particle-size-tunable band gap PL, from the near- to the mid-IR. The transferability from aqueous to organic solvents is greatly improved and facilitated by using MEA as initial stabilizer. The various surface functionalities

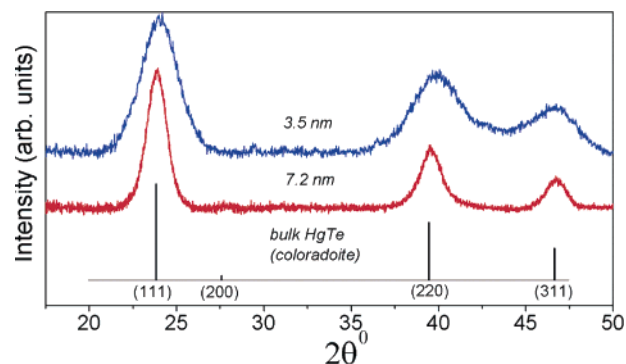


Figure 3. XRD patterns of 3.5 and 7.2 nm HgTe NCs. The XRD spectrum of bulk HgTe¹¹ (coloradoite) is presented for comparison.

(hydrophobic and hydrophilic) of the HgTe NCs together with their emission in the spectral range from the telecommunications to the molecular vibrations make them very promising for applications in infrared optical devices, such as NC-sensitized polymer solar cells,¹³ microcavity light emitters,¹⁴ or molecule detection systems.

Acknowledgment. Financial support from the Austrian Science Foundation FWF (START Project Y179 and SFB-IRON) and the GME is gratefully acknowledged. TEM images were taken at the Technical Service Unit of Johannes Kepler University.

Supporting Information Available: Experimental details, TEM and SAED data. This material is available free of charge via the Internet at <http://pubs.acs.org>.

References

- (1) (a) Alivisatos, A. P. *Science* **1996**, *271*, 933–937. (b) Murray, C. B.; Norris, D. J.; Bawendi, M. G. *J. Am. Chem. Soc.* **1993**, *115*, 8706–8715. (c) Hines, M. A.; Guyot-Sionnest, P. *J. Phys. Chem. B* **1998**, *102*, 3655–3657. (d) Peng, X.; Schlamp, M. C.; Kadavanich, A. V.; Alivisatos, A. P. *J. Am. Chem. Soc.* **1997**, *119*, 7019–7029.
- (2) (a) Murray, C. B.; Sun, S.; Gaschler, W.; Doyle, H.; Betley, T. A.; Kagan, C. R. *IBM J. Res. Dev.* **2001**, *45*, 47–55. (b) Hines, M. A.; Scholes, G. D. *Adv. Mater.* **2003**, *15*, 1844–1849. (c) Battaglia, D.; Peng, X. *Nano Lett.* **2002**, *2*, 1027–1030.
- (3) (a) Eisler, H. J.; Sundar, V. C.; Bawendi, M. G.; Walsh, M.; Smith, H. I.; Klimov, V. *Appl. Phys. Lett.* **2002**, *80*, 4614–4616. (b) Kazes, M.; Lewis, D. Y.; Ebenstein, Y.; Mokari, T.; Banin, U. *Adv. Mater.* **2002**, *14*, 317–321.
- (4) Bruchez, M.; Moronne, M.; Gin, P.; Weiss, S.; Alivisatos, A. P. *Science* **1998**, *281*, 2013–2016.
- (5) Michler, P.; Imamoglu, A.; Mason, M. D.; Carson, P. J.; Strouse, G. F.; Buratto, S. K. *Nature* **2000**, *406*, 968–970.
- (6) Pietryga, J. M.; Schaller, R. D.; Werder, D.; Stewart, M. H.; Klimov, V. I.; Hollingsworth, J. A. *J. Am. Chem. Soc.* **2004**, *126*, 11752–11753.
- (7) Böer, K. W. *Survey of Semiconductor Physics: Electrons and Other Particles in Bulk Semiconductors*; Van Nostrand Reinhold: New York, 1990; Chapter 9.
- (8) Rogach, A.; Kershaw, S.; Burt, M.; Harrison, M.; Kornowski, A.; Eychmüller, A.; Weller, H. *Adv. Mater.* **1999**, *11*, 552–555.
- (9) Kuno, M.; Higginson, K. A.; Qadri, S. B.; Yousuf, M.; Lee, S. H.; Davis, B. L.; Mattoussi, H. *J. Phys. Chem. B* **2003**, *107*, 5758–5767.
- (10) (a) Green, M.; Wakefield, G.; Dobson, P. J. *J. Mater. Chem.* **2003**, *13*, 1076–1078. (b) Brennan, J. G.; Siegrist, T.; Carroll, P. J.; Stuczynski, S. M.; Reynnders, P.; Brus, L. E.; Steigerwald, M. L. *Chem. Mater.* **1990**, *2*, 403–406.
- (11) JCPDS database of International Center for Diffraction Data Card 32-0665.
- (12) Gaponik, N.; Talapin, D. V.; Rogach, A. L.; Eychmüller, A.; Weller, H. *Nano Lett.* **2002**, *2*, 803–806.
- (13) Günes, S.; Neugebauer, H.; Saricifci, N. S.; Roither, J.; Kovalenko, M.; Pillwein, G.; Heiss, W. *Adv. Funct. Mater.* In press.
- (14) Roither, J.; Kovalenko, M. V.; Pichler, S.; Schwarzl, T.; Heiss, W. *Appl. Phys. Lett.* **2005**, *86*, 241104.

JA058440J